Pergamon

Journal of Structural Geology, Vol. 18, Nos 2/3, pp. 217 to 234, 1996

0191-8141/96 $15.00 + 0.00

0191-8141(95)E112-3

The structural evolution of active fault and fold systems in central Otago, New Zealand: evidence revealed by drainage patterns

JAMES JACKSON

Bullard Laboratories, Madingley Road, Cambridge CB3 0EZ, U.K.

and

RICHARD NORRIS and JOHN YOUNGSON

Department of Geology, University of Otago, P.O. Box 56, Dunedin, New Zealand

(*Received* 28 *December* 1994; *accepted in revised form* 22 *August* 1995)

Abstract—Central Otago in New Zealand is an area of active continental shortening in which a peneplain surface cut into schist has been deformed by folds, which are developed above buried reverse faults. We use the drainage patterns in this region to demonstrate various processes in fold (and fault) growth and interaction that would be difficult to identify by other means. In particular we show: (1) how simple asymmetric folds can develop into box folds; (2) how apparently continuous ridges were formed by the coalescing of quite separate propagating fold (and fault) segments; (3) evidence for the relative ages (or relative uplift rates) of adjacent structures; and (4) evidence for the propagation direction of folds (or faults) as they grow. The few quantitative estimates we obtain for fault propagation rates suggest an increase in length of 10–50 m per earthquake on faults about 20 km long. These estimates are very uncertain, but are similar in magnitude to an estimate made in Nevada for a normal fault of similar size and are also similar to predicted estimates from theoretical growth models. They raise the question of whether fault growth, earthquake recurrence rates and climate change can interact to produce semi-regular discrete features in an active landscape.

INTRODUCTION

In regions of active continental shortening topography can be generated rapidly compared with rates of erosion and deposition, so that the position of ridges and range fronts is often a useful guide to the location of active faults and folds (e.g. Cotton 1917, Stein & Yeats 1989). The landscape then evolves as tectonically-produced slopes are modified by erosion and deposition as well as by the continued growth of active structures. Drainage systems adapt to changes in the surface slope and thus have the potential to record information about the evolution of faults and folds (e.g. Cotton 1942, Ollier 1981, Leeder & Jackson 1993). In this paper we examine the drainage systems associated with active reverse faults and folds in central Otago, New Zealand. We show that drainage patterns and their evolution reveal evidence for the growth of these structures and the interactions between them that would be difficult to obtain by conventional geological methods (such as the dating of sedimentary material). This is particularly the case in the emerging hangingwalls or anticlines, where the environment is essentially erosional.

The hypocentres of most reverse-faulting earthquakes on the continents are restricted to the upper 15–20 km of the crust. Since the geomorphological features we describe are best displayed by large structures, all the faults we discuss here are 15–30 km in length and therefore have dimensions that are comparable with the thickness of the seismogenic layer. Such structures can generate earthquakes of $\mathbf{M}_w$ 6–7 (e.g. Shimazaki 1986). Most reverse-faulting earthquakes of this size occur on relatively steeply dipping (30–60°) faults (e.g. Molnar & Chen 1982), though ones with lower dips are also known. Fault rupture in such earthquakes often fails to reach the surface and leads instead to the uplift of an anticline above the buried reverse fault (e.g. King & Vita-Finzi 1981, Stein & King 1984, Yeats 1986, Philip *et al.* 1992). In such cases the growth of the anticline is clearly related to the increased slip on its underlying fault.

As faults increase their displacement through repeated earthquakes they are also likely to grow in length. The simplest argument supporting this assertion comes from two observations: (1) that the ratio of slip to rupture length in an earthquake is typically 10^{-5}–10^{-4}; and (2) that the ratio of total displacement to length on geological faults is typically 10^{-3}–10^{-1}. If these two relations are to be true simultaneously, then faults must increase in length as they increase in displacement (e.g. Watterson 1986). Several theoretical models of fault growth have been developed that attempt to reconcile these empirical observations (e.g. Watterson 1986, Walsh & Watterson 1988, Cowie & Scholz 1992, Gillespie *et al.* 1992, Scholz *et al.* 1993), but actual observations of fault growth in the field remain rare. Jackson & Leeder (1994) presented geomorphological evidence for the increase in length with time of a 30 km-long active normal fault in Nevada. Like the theoretical models referred to above, Jackson & Leeder (1994) assumed that the fault moves only in earthquakes whose size is determined by the total length of the fault segment that

is available for rupture. They then estimated a rate of increase in fault length of about 50 m per earthquake, which is similar to that predicted by the theoretical growth models. This perhaps explains why observations of growth are rare: it is very improbable that an increment in length of this amount would be noticed after an individual earthquake, even if surface rupture in both that earthquake and in the previous one were clear. Moreover, with the repeat times of large earthquakes typically measured in hundreds or thousands of years, the chances of finding sufficient dateable material to demonstrate incremental fault growth over a few earthquake cycles must be slim. We believe the evolution of the drainage and geomorphology associated with changing tectonic slopes offers a better chance of observing fault growth, which was a motivation for this study.

Recent theoretical fault growth models have concentrated on the increase in length of individual fault segments (e.g. Gillespie *et al.* 1992, Scholz *et al.* 1993). Faults can also increase their length by coalescing with neighbouring segments (e.g. Trudgill & Cartwright 1994, Wu & Bruhn 1994, Dawers & Anders 1995), which is a phenomenon we also demonstrate here.

GEOLOGICAL SETTING OF CENTRAL OTAGO

Central Otago (Fig. 1) lies east of the Southern Alps in the South Island of New Zealand. It is an elevated region (500–1000 m) of relatively gentle topography, whose dominant geomorphological feature consists of a peneplain surface that is flat except where it is warped or broken into a series of parallel ridges and valleys by folds and reverse faults trending NE–SW. These structures are active but accommodate only a few mm a^{-1} of the 35–45 mm a^{-1} oblique convergence between the Pacific and Australian plates, most of which is taken up on or near the Alpine Fault west of the much higher (2000–3000 m) Southern Alps (Norris *et al.* 1990, Berryman *et al.* 1992, Bishop 1994).

In the area of our study the Otago peneplain is developed on the Otago Schist (Mortimer 1993) and represents a prolonged period of regional erosion of probably diachronous age between Late Cretaceous and Miocene. The peneplain was initially covered by mostly non-marine sediments of Late Cretaceous to Miocene age. These sediments have been widely stripped off the basement schist by regional uplift accentuated in places by folding and reverse faulting to re-expose the peneplain surface beneath. Locally both Cenozoic and Quaternary sediments are preserved in basins formed by synclines or footwall blocks. The peneplain surface is often, but not always, sub-parallel to the well-developed schistosity in the Otago Schist. Areas of marginally degraded peneplain are commonly indicated by scattered 'sarsen stones', which are the remnants of a resistant silica-cemented layer formed during diagenesis within quartz-rich Late Cretaceous to Tertiary sediments that overlie the schist (e.g. Cotton 1917).

The peneplain provides a reference surface for evaluating the Late Cenozoic deformation in Otago, and has been used for this purpose by Bishop (1974, 1994), Suggate (1978) and Stirling (1990), among others. For our purposes it is also useful in that the schist in which it is developed forms all the uplifted anticlines or hanging-walls we discuss. There are no significant differences in the textural grade of the schist between the range tops and the valleys, and the ranges are made of similar grade schist (textural grade 3–4 of Mortimer 1993) over the whole area we consider. Variations in geomorphology between these ridges thus reflect their structural development, rather than their different susceptibilities to erosion. Cotton (1917, 1942) realized that the drainage on the ridges in central Otago was consequential on their structural development: i.e. that the stream patterns were established in the Tertiary sediments and superimposed on the emergent schist as it was exposed through uplift and erosion. Cotton's insights were very substantial, but he was working at a time when seismological knowledge was primitive, and in particular the relations between faulting and earthquakes were insufficiently understood to pose the questions about fault growth and interaction that are the subject of this paper.

The range fronts in central Otago are often abrupt and linear, especially on satellite images (e.g. Yeats 1987, Madin 1988) and appear on many maps as faults (e.g. Mortimer 1993). Faults undoubtedly do outcrop along the flanks of several ranges and trenching has demonstrated their Late Quaternary activity (e.g. Beanland *et al.* 1986, Beanland & Barrow-Hurlbert 1988, Beanland & Berryman 1989, Berryman & Beanland 1991). However, it is also clear from the warping of the peneplain surface and the changing orientation of the schistosity that folding has played an important part in the uplift of the ranges. The regular parallel layering in the schist certainly makes it susceptible to folding. However, the relative importance of faulting and folding at the surface is not significant in this study, since it is virtually certain, based on well-studied analogues elsewhere (e.g. King & Vita-Finzi 1981, Stein & King 1984, Hauksson *et al.* 1988, Philip *et al.* 1992), that all these anticlines are underlain at shallow depths by reverse faults. Sometimes, particularly along some of the higher and more developed ranges, faulting reaches the surface close to the folded unconformity between the peneplain and the preserved Tertiary sediments that follows the range front. Along some of the smaller range fronts there are no obvious signs of Late Quaternary faulting at the surface. For our purposes it is sufficient to note our assumption that the growth of the anticline ridges intimately reflects the growth of the reverse faults we presume lie beneath them, and there is no significance to whether we refer to the ridges as faults or folds: we use both interchangeably.

Central Otago lies in the rain shadow of the Southern Alps with respect to the prevailing westerly winds that cause high rainfall and erosion on the west coast of the South Island. Although relatively dry, it is subject to the maritime climate of the east coast, which brings some rain. There is no evidence for Late Quaternary ice sheets

or ice-based erosion on the ridge systems we discuss here, which are at relatively low elevations. Patterned ground on the Rock and Pillar Range (McCraw 1965, McSaveney & Stirling 1992) suggests some local permafrost conditions while glaciation affected the Southern Alps.

We first look at the drainage associated with simple isolated anticlinal structures that are relatively two-dimensional, though they do have identifiable ends. We then look at structures which the drainage demonstrates are not two-dimensional but are formed of separate segments that have either now coalesced or are arranged in an en echelon stepping fashion. Finally, we examine how the drainage systems provide evidence of the interaction between adjacent structures; revealing how they attained their present configuration through propagation and growth.

SIMPLE STRUCTURES IN ISOLATION

Taieri Ridge

The smallest amplitude (~300 m), lowest (~650 m) and simplest of the ridges we discuss is Taieri Ridge in the southeast of our study area (Fig. 1). It is an asymmetric anticline, with its southeast side steeper than its northwest. The ridge axis is horizontal in its central part but is inclined gently to the southwest at its southwest end. To the northeast the ridge merges with a roughly horizontal less-deformed area of the peneplain surface. The drainage system on the anticline mirrors its structure and asymmetry precisely (Figs. 2a & b and 3). There is a clear drainage divide along the ridge, situated close to the steeper southeast flank. The consequent streams flow perpendicular to both the drainage divide and the structural contours on the peneplain surface. There is a hint of a radial drainage pattern around the plunging nose of the anticline in the southwest, but this has been disturbed by the two large longitudinal streams (the Taieri River and Sheepwash Creek) that flow parallel to the ridge and gather the catchment off it. The half-wavelength of the fold is the order of 15 km: typical of a fold above a steep reverse fault that cuts through most of the 10–15 km thick seismogenic upper crust (e.g. Ruegg *et al.* 1982). The asymmetry of the fold indicates that the underlying fault dips to the NW. The exposed length of the ridge is about 20 km, thus the underlying fault is capable of generating an earthquake of about $\mathbf{M}_w$ 6.0–6.5 (see e.g. Shimazaki 1986).

The Rock and Pillar Range

By contrast, the Rock and Pillar Range, which lies adjacent and to the northwest of Taieri Ridge, has a larger amplitude (~1000 m), is higher (~1200 m) and is broadly symmetric in shape, with a box-like cross section (Figs. 2c & d and 3a). It has steep flanks on both the southeast and northwest sides with an almost flat central part. Evidence for reverse faulting occurs locally along the southeast margin, but displacements on outcropping faults at the surface are probably small compared to the displacement at depth needed to produce the relief on the range itself (Salton 1993). Although the structure of the Rock and Pillar Range appears roughly symmetric, its drainage system is very asymmetric. The drainage divide is located close to the southeast margin, across which there is a simple system of closely-spaced streams flowing perpendicular to the divide and to the structural contours, as on Taieri Ridge. Much larger streams emerge along the northwest flank, draining the entire central area of the range as far east as the divide. These streams cut prominent gorges through the central flat part of the box fold (Fig. 3). The drainage systems on the Rock and Pillar Range indicate that the symmetric box fold grew from an originally asymmetric fold which established the drainage divide along the southeast flank, similar to that of Taieri Ridge. The northwest flank was later elevated and steepened, requiring the streams draining northwest to cut down and make gorges. These streams, being longer, with greater catchment and erosive power, have produced a more complex pattern of captured streams in the central part of the fold northwest of the drainage divide. There is a well-developed radial drainage pattern around the northeast end of the range.

We presume that the underlying structures responsible for the drainage pattern are a reverse fault dipping NW along the southeast margin of the range, followed by a later reverse fault dipping SE along the northwest margin (Fig. 2d). The two steep flanks are about 20 km apart, so that the two reverse faults, if they both dipped at 45°, would intersect towards the base of the seismogenic layer at ~10 km: but we have no constraint on the actual dips of the faults.

The drainage patterns in Fig. 2 indicate how a simple asymmetric fold like Taieri Ridge can evolve into a larger box fold like the Rock and Pillar Range by the development of a later backthrust in the hangingwall of the initial fault. In this case, with the uplifted range all of a uniform lithology, it is difficult to see how this information could be obtained in any way other than from the drainage pattern.

SEGMENTED RANGES

It is common for reverse fault systems and their accompanying hangingwall anticlines to be segmented along strike. This means that long, apparently continuous faults actually consist of several discrete fault segments that are distinguished by small lateral offsets (usually less than about 5 km) or by changes in strike or dip. The segmentation of the fault system has a profound effect on rupture propagation during earthquakes as slip on one segment may or may not trigger rupture on the next. The discontinuous rupture history can be seen in the seismograms of the earthquake and it is sometimes possible to correlate discrete sub-events with particular

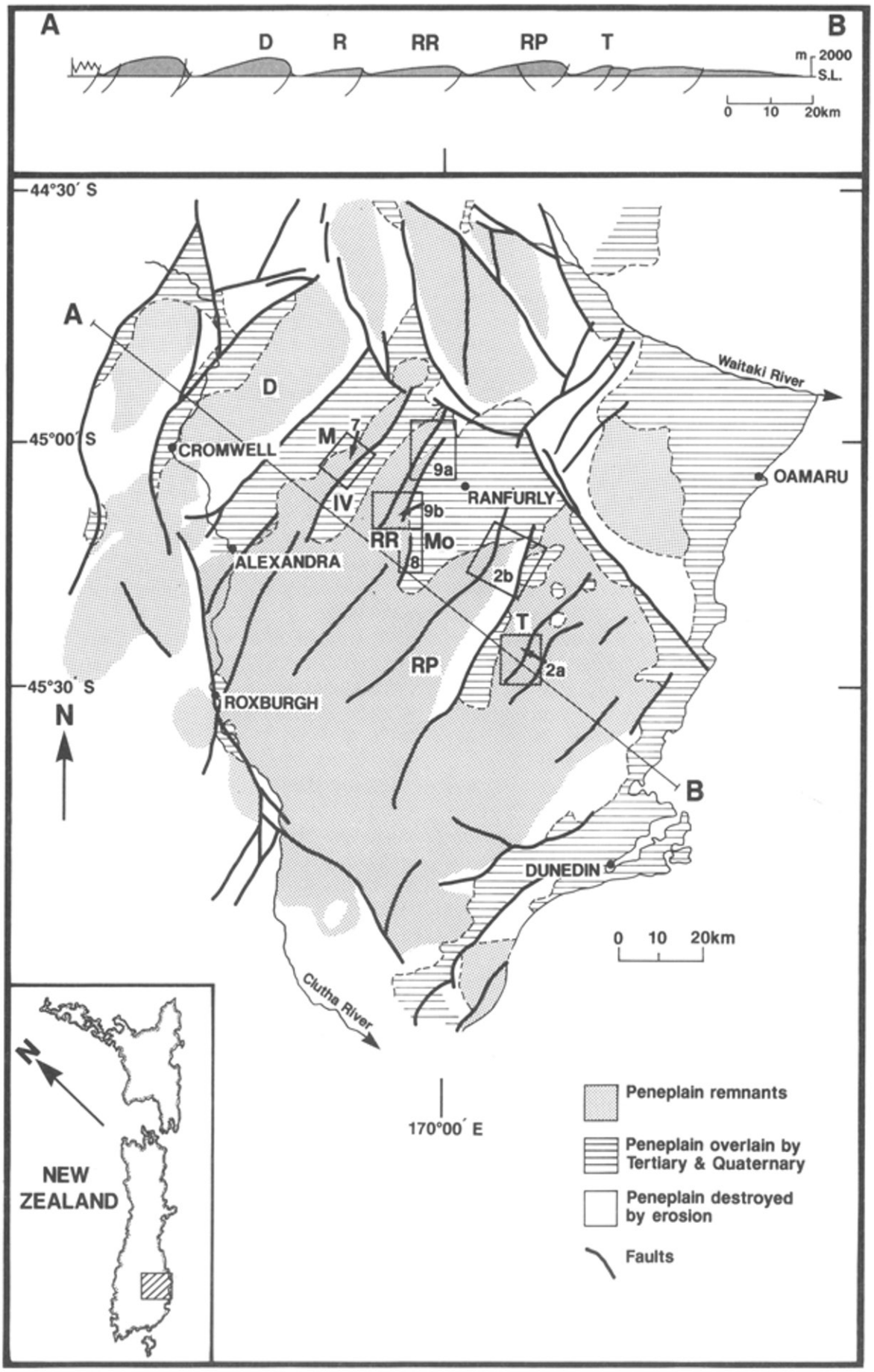

Fig. 1. (a) Location map of the Otago peneplain, modified from Bishop (1994). 'Faults' are taken from Mortimer (1993): in the areas we discuss these are mainly the steep limbs of asymmetric folds, and there is little evidence of faulting at the surface. D, Dunstan Range; R, Raggedy Range; ; RP, Rock and Pillar Range; T, Taieri Ridge; RR, Rough Ridge; M, Manuherikia valley; IV, Ida Valley; Mo, Maniototo depression. The areas of Figs. 2, 7, 8 and 9 are outlined by boxes.

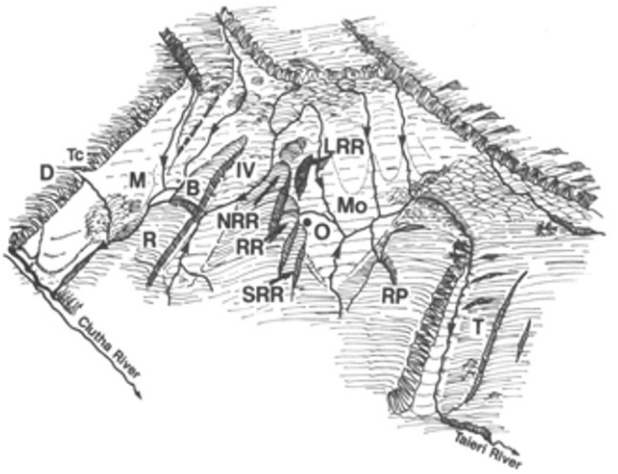

Fig. 1. (b) Generalized cartoon looking north over the topography and drainage of Central Otago, modified from Cotton (1917). Places identified by letters are those in (a), with the additions: Tc, Thompsons Creek; B, Blackstone Hill; O, Oliverburn; NRR, North Rough Ridge; SRR, South Rough Ridge; LRR, Little Rough Ridge.

fault segments visible at the surface (e.g. Yielding 1985, Pacheco *et al.* 1989, Philip *et al.* 1992).

As each fault segment evolves semi-independently it can produce substantial structural variations along strike in the hangingwall and footwall of the fault system as a whole. These structural variations can in turn control variations in sediment thickness and supply along the strike of elongated fault-bounded basins. Studies of this aspect of fault segmentation have concentrated particularly on normal faults (e.g. Schwartz & Coppersmith 1984, Leeder & Gawthorpe 1987, Roberts & Jackson 1991), partly because of the economic importance of syn-rift sediment deposits and also because segment boundaries are often clearly revealed by the geomorphology and drainage (e.g. Crone & Haller 1991, Leeder & Jackson 1993). Reverse faults have attracted less attention, so we now show an example where the drainage systems can reveal fault segmentation and also how that segmentation has evolved with time.

Raggedy Range and Blackstone Hill

The Raggedy Range in the southwest and Blackstone Hill in the northeast form an elongate ridge ~30 km long (Fig. 1). The Ida Valley, which lies southeast of the ridge, is drained by the Ida Burn and Pool Burn, which coalesce and flow through a gorge occupying a saddle that separates Raggedy Range from Blackstone Hill. Either side of the saddle the ridge is asymmetric in cross

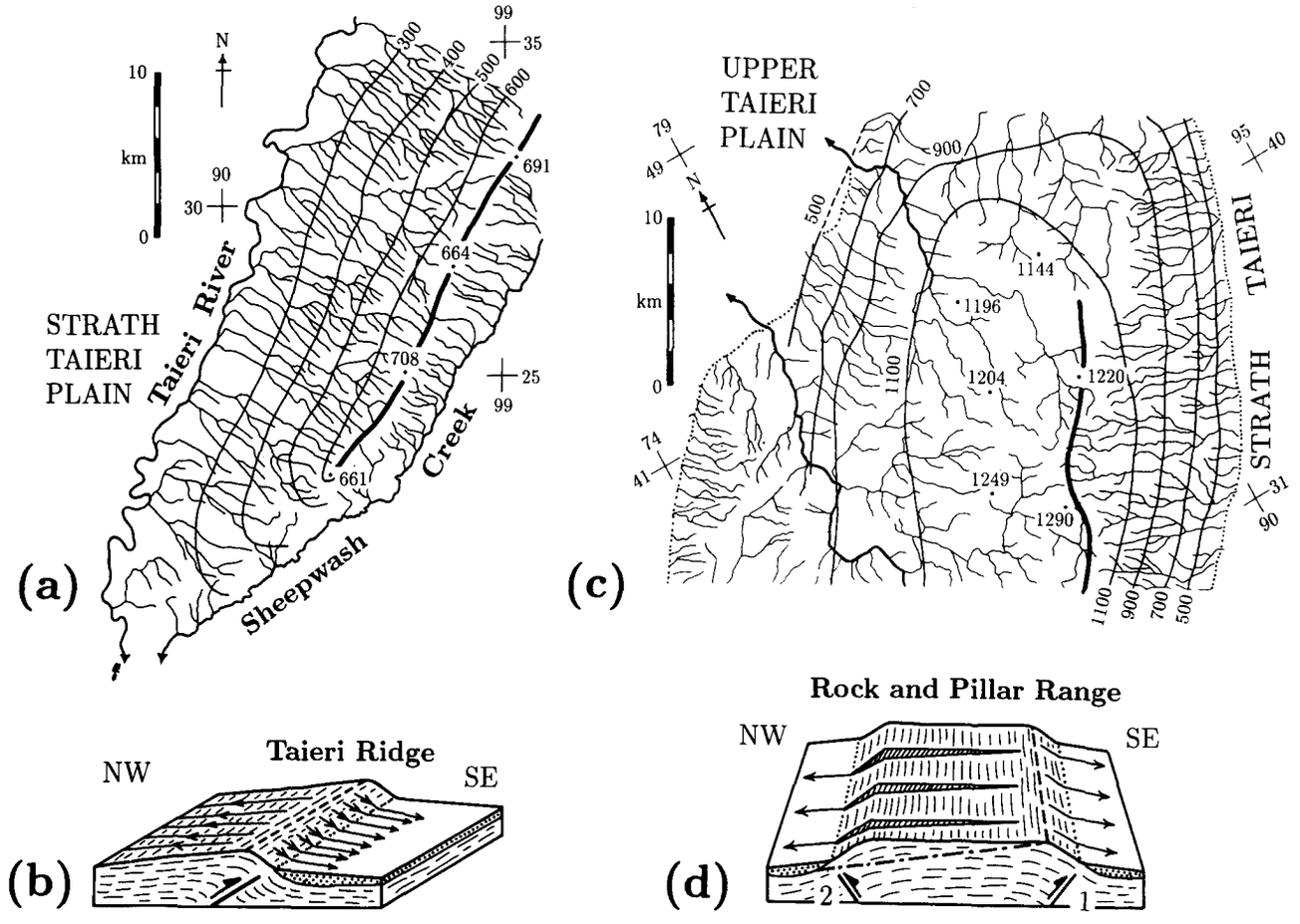

Fig. 2. (a) Drainage map and structural contours on the peneplain surface for Taieri Ridge (see Fig. 1). Spot heights and contours are in metres. The thick black line marks the main drainage divide. (b) Simplified cartoon showing the structure of Taieri Ridge and its relation with the drainage and presumed underlying fault. (c) Drainage and structural contour map of the northern end of the Rock and Pillar Range (see Fig. 1). The line of dots at the foot of the minor drainage marks the base of the range front. (d) Simplified cartoon illustrating the structure and drainage of the Rock and Pillar Range. We surmise that an early fault (1) produced an asymmetric range profile (dot–dash line) that was later steepened by a second fault (2).

section, with the drainage divide closer to the steeper southeast flank. We show below that the drainage system, particularly in the region of the saddle (Figs. 3b and 7), indicates that Blackstone Hill and Raggedy Ridge evolved as quite separate anticlines, we presume above distinct reverse fault segments at depth, that have now coalesced to form a single longer ridge.

Blackstone Hill is a ridge 800–900 m high (400–500 m above its adjacent valleys) with a pronounced nose at its southwest end forming the saddle occupied by the Ida Burn gorge. The saddle is well defined by the structural contours on the peneplain surface, and sarsen stones are found close to and within 100 m elevation of the gorge itself, indicating that the saddle is a genuine undulation in the peneplain surface and not an erosional feature. The southwest nose of the Blackstone Hill ridge also has a well-developed radial pattern in its consequent streams. The topography of Blackstone Hill is somewhat box-like in cross section, resembling a smaller version of the Rock and Pillar Range, and this tendency to symmetry is seen also in the structural contours on the peneplain surface (Fig. 7a). The northwest flank has been steepened by later SE-dipping reverse faults, some of which are observable in abandoned gold workings. Note, however, that the scale here is smaller than the Rock and Pillar Range, as the Blackstone Hill ridge is only 6–10 km wide. If the controlling faults at depth dip at around 45°, the later SE-dipping fault would meet the earlier NW-dipping fault at shallow depths (3–5 km).

The ridge of the Raggedy Range is lower in elevation (500–600 m), smaller in amplitude (100–200 m) and more pronounced in its asymmetry. At its northeast end it plunges towards the saddle of the Ida Burn gorge, but does not show the pronounced radial drainage system seen at the southwest end of Blackstone Hill. Instead there are two prominent air gaps in the ridge, marking the former courses of streams that crossed what is now the divide. The most obvious is just 2 km southwest of the present Ida Burn gorge (Figs. 3b and 7a & b) and is a broad open valley, once occupied by a major river and now filled with gravel, that is dry in its central part and in its northwest part is occupied by stream channels far too small to have formed it. This broad dry valley crosses the divide to the southeast where it is truncated as a hanging valley by a smaller, later consequent stream flowing down the southeast flank of the anticline (Fig. 4). This air gap is clearly an old course of the Pool Burn that crossed the line of the ridge in a gorge at this point and has since been abandoned as the ridge was uplifted. The old entrance to the gorge is preserved on the southeast ridge flank at Slogarie Farm, where it is still at approximately the elevation of the current Pool Burn. The highest part of the abandoned channel is now 100 m above the old gorge entrance.

Three kilometres farther southwest is another large air gap (marked by an open circle in Fig. 7a), less well preserved than the former, and still more air gaps are seen even farther southwest along the Raggedy Range (beyond the bottom of Fig. 7a), which continues for about 15–20 km southwest of the present Ida Burn gorge. The longitudinal drainage on the northwest side of the Raggedy Range–Blackstone Hill ridge is channelled in the Manuherikia River, which is deeply entrenched in the Lauder gorge on the northwest flank of the Raggedy Range (Fig. 7a).

The drainage pattern suggests the following evolutionary history of the structures, illustrated in Fig. 7(c). The air gaps at the northeast end of the Raggedy Range indicate that a stream, probably the Pool Burn, used to cross the ridge at points south of the present Ida Burn gorge, but has been progressively pushed northeast by the rising ridge of the Raggedy Range as it grew in that direction. Prior to the growth of the Raggedy Range most of the drainage in the southern Ida Valley probably flowed directly across the line of the present ridge to join the Manuherikia River. The northeastward course of the Pool Burn is anomalous as most of the longitudinal drainage in this region flows southwest to join the Clutha River (Fig. 1). The rising of the Raggedy Range and its northeastward growth may have been responsible for forming the Pool Burn and causing it to flow northeast round the nose of the growing anticline to join the main Manuherikia River, which flows southwest. The lack of air gaps and the radial drainage pattern at the southwest end of Blackstone Hill shows that it had a different history: the Ida Burn was always able to flow around the end of this rising Blackstone Hill ridge without entrenching in a gorge, presumably because it was already flowing southwest down the regional slope to the Clutha River and was uninhibited by the Raggedy Range which did not then exist. Thus, it is the northeastward growth of the Raggedy Range that has trapped the coalesced Ida Burn and Pool Burn into the saddle where the two ridges meet, now occupied by the present Ida Burn gorge. The air gaps south of the present gorge were occupied by either the coalesced Ida and Pool Burns or by the Pool Burn alone. They were probably occupied by the Pool Burn alone, because the stream concerned had insufficient power to maintain the gorge in the presence of the rising anticline, whereas the Ida and Pool Burns together are now clearly able to do so. But this is not a unique interpretation as erosive power and sediment yield can change with climate and other factors. However, it is hard to see how the present geometry could arise unless the Ida Burn was already flowing round the end of Blackstone Hill before the northward growth of Raggedy Range caused it to join with the Pool Burn. Thus we suggest that Blackstone Hill was formed before the emergence of the northeast end of the Raggedy Range.

The limited erosion of the Manuherikia River into the northwest flank of Blackstone Hill and, more dramatically, into the Lauder gorge on the northwest flank of the Raggedy Range, suggests that these two ridges rose after the Manuherikia River had established its position (see also McSaveney & Stirling 1992). The Manuherikia receives the outwash from the Dunstan Range (Fig. 1), which at 1600 m is the highest ridge in the area we consider. It is an asymmetric anticline with a steep southeast flank, and is composed of two segments separated by a saddle through which Thompsons Creek

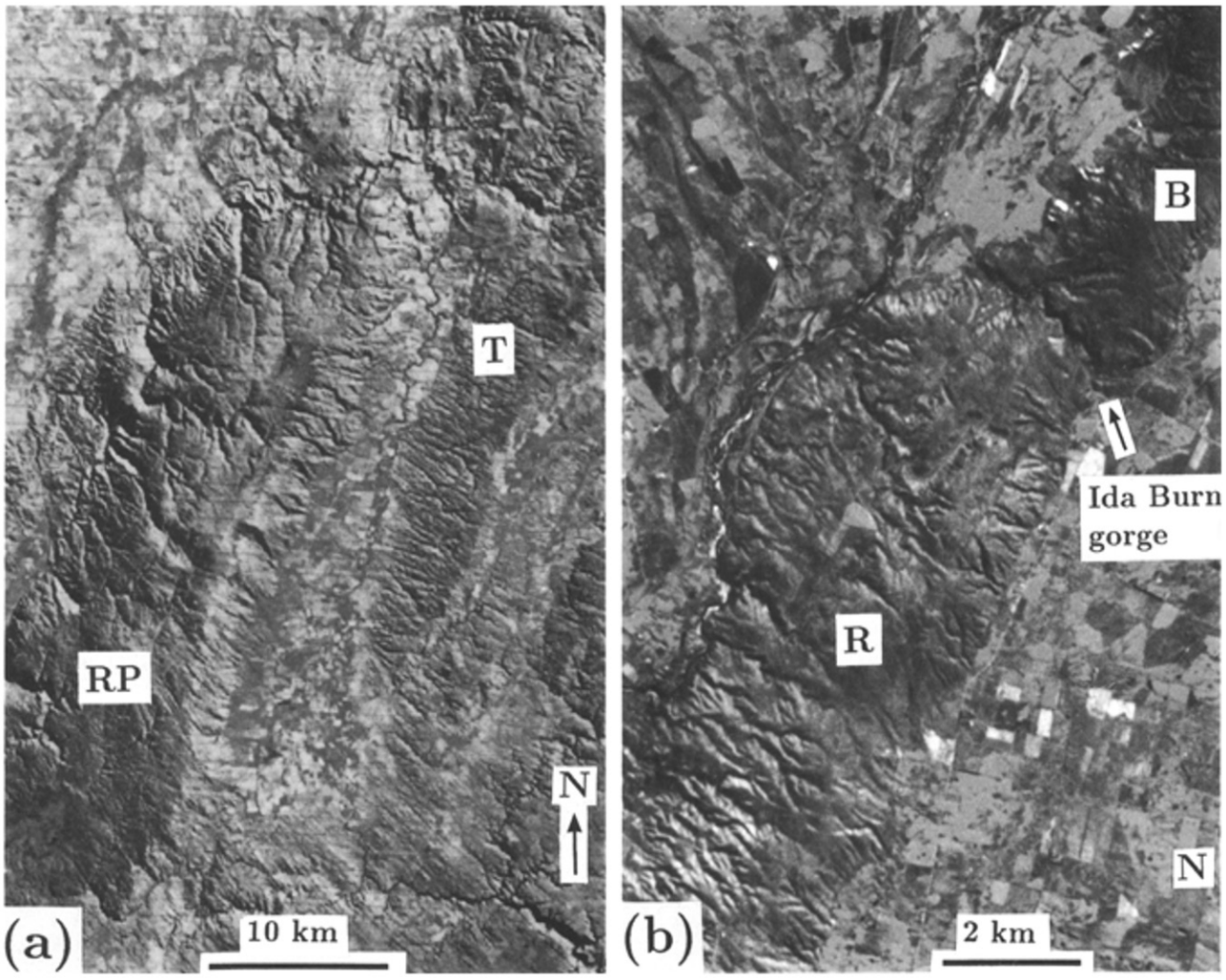

Fig. 3. (a) LANDSAT image of the Rock and Pillar Range (RP) and Taieri Ridge (T). See Figs. 1(b) and 2. (b) SPOT image of the Ida gorge between Raggedy Range (R) and Blackstone Hill (B). See Figs. 1(b) and 7.

Fig. 4. Southeast end of the dry valley that marks the former position of a major gorge through the Raggedy Range at Slogarie. The view is to the northwest, taken 1 km northwest of Slogarie Farm. The broad open dry valley in the centre of the picture is cut in the foreground by a steep consequent stream on the southeast flank of Raggedy Range, leaving a hanging valley.

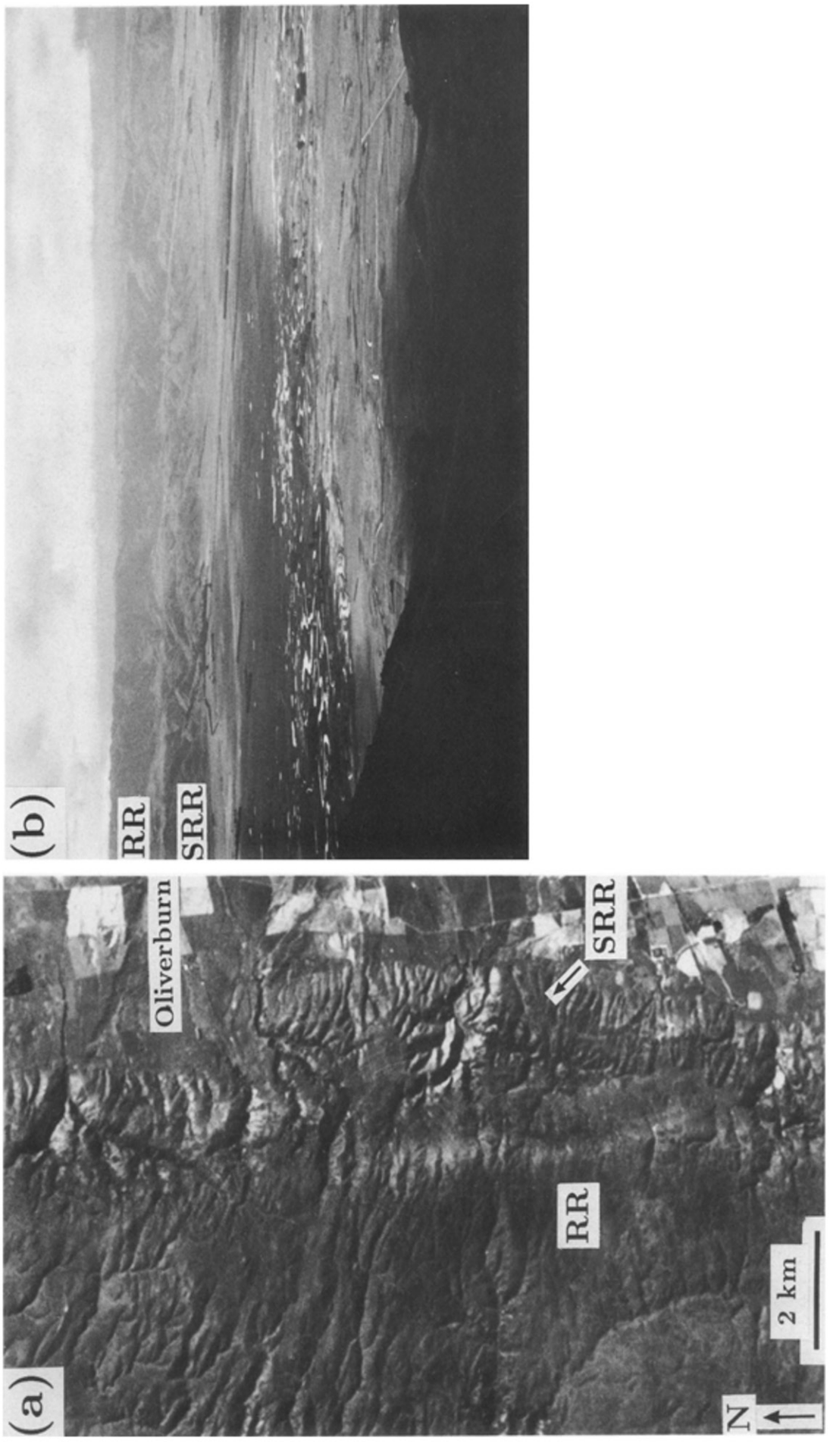

Fig. 5. (a) SPOT image of the step between Rough Ridge (RR) and South Rough Ridge (SRR) at Oliverburn. See Figs. 1(b) and 8. (b) View west over the upper Taieri plain from Ewe Hill (grid ref 400N 765E on Fig. 2c) on the Rock and Pillar Range. The frontal ridge is South Rough Ridge (SRR), decreasing in height to the right (north). In the background is the higher Rough Ridge (RR). Oliverburn is just off the right edge of the picture (see Fig. 8a).

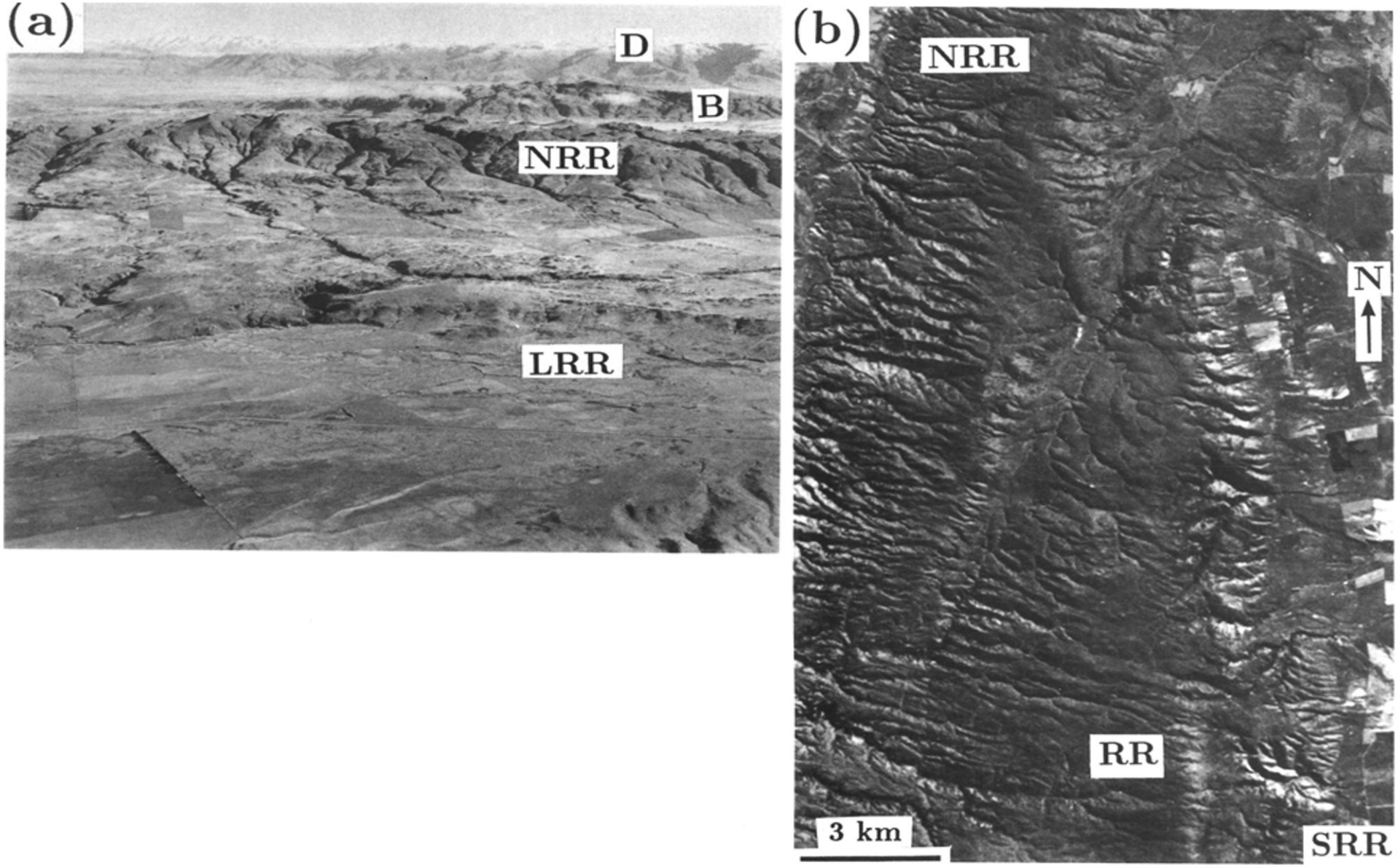

Fig. 6. (a) View northwest across Little Rough Ridge (LRR, small scarp in foreground), North Rough Ridge (NRR) and Blackstone Hill (B) to the Dunstan Range (D, background). See Figs. 1(b) and 9(a). Photograph: Lloyd Homer. (b) SPOT image of the Rough Ridge (RR)–North Rough Ridge (NRR) overlap. See Figs. 1(b) and 9.

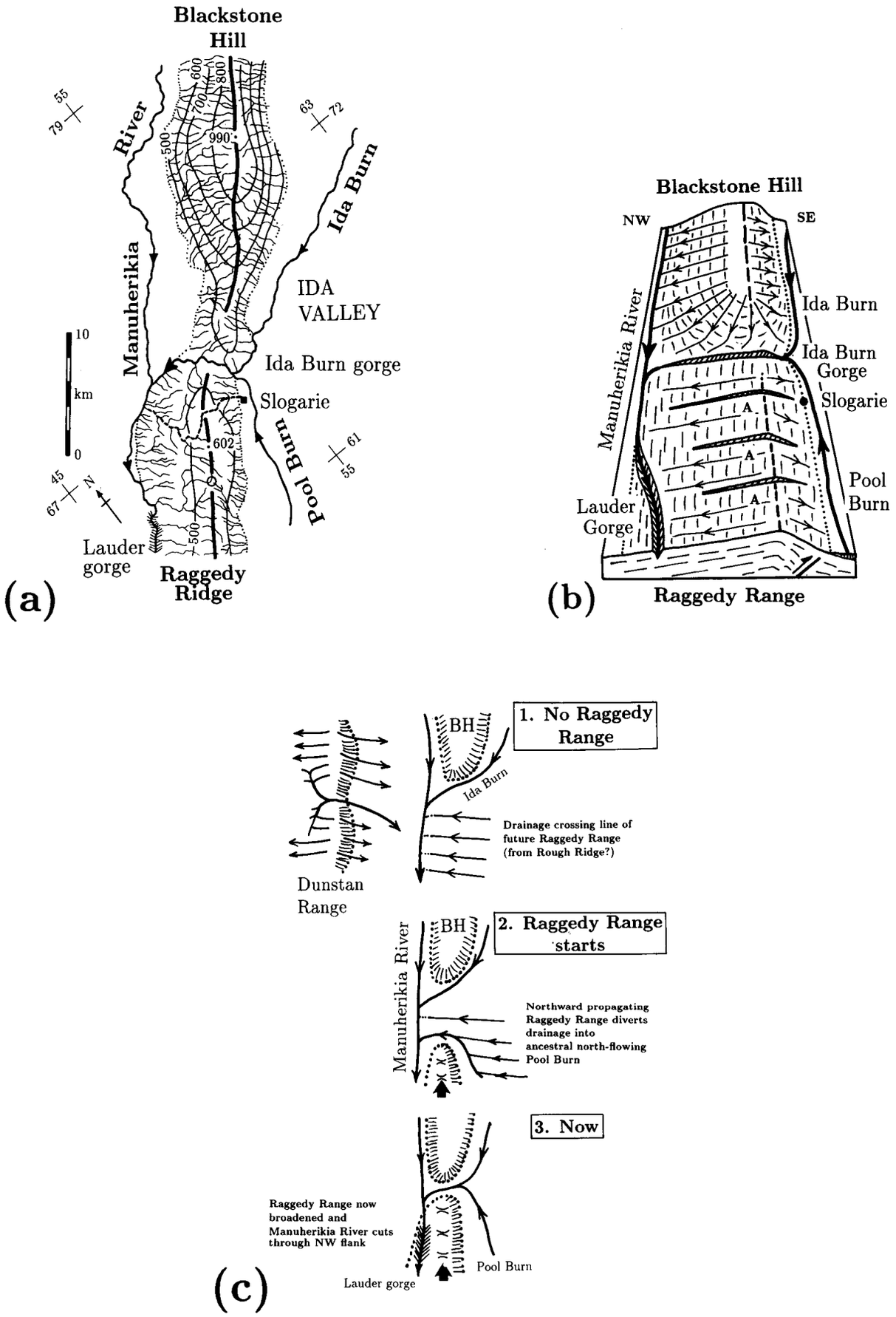

Fig. 7. (a) Drainage map and structural contours for the Ida Burn gorge region between Raggedy Range and Blackstone Hill (see Fig. 1). Symbols as in Fig. 2. The course of the old gorge at Slogarie is shown by dashes (see Fig. 4). An air gap south of this is marked with an open circle. (b) Schematic block diagram looking northeast along the Raggedy Range and Blackstone Hill. Blackstone Hill has a radial drainage pattern at its southwest end. Raggedy Range has a series of dry air gaps (marked A) southwest of the present Ida Burn Gorge. The largest of these is by Slogarie Farm (Figs. 3b and 4). (c) Schematic illustration of the evolution of the structures and drainage in the Raggedy Range–Blackstone Hill region.

disgorges. Several Late Quaternary fault scarps outcrop at or near the base of the southeast flank of the range (Beanland *et al.* 1986), though the main topographic expression of the range is created by folding. Large alluvial fans have been deposited on the piedmont at the foot of the southeast flank (Madin 1988) and it is these that have caused the Manuherikia River to flow at some distance from the range front. Most of the Manuherikia's course is through sediment, but its catchment is large and its erosive power sufficient for it to maintain its gorge through the uplifting schist on the northwest flank of the Raggedy Range.

Our preferred interpretation of the drainage is that the Dunstan Range rose first, followed by Blackstone Hill and then the Raggedy Range. This is not a unique interpretation because we cannot distinguish between different relative ages and different relative rates of uplift. So the proposed chronological order could instead be an order of relative slip rates on the underlying faults. Either way, it is clear that the apparently continuous ridge formed by the Raggedy Range and Blackstone Hill evolved from the coalescing of two independent segments that grew towards each other.

INTERACTIONS BETWEEN SEGMENTS

Where normal fault segments are arranged in an en echelon system along strike, the drainage characteristics in the steps between segments can indicate how the system is evolving (e.g. Jackson & Leeder 1994). We now demonstrate that the same is true of en echelon reverse faults or anticlines, by looking at the Rough Ridge system, which lies between the Rock and Pillar and the Raggedy Range–Blackstone Hill ridges (Fig. 1). The Rough Ridge system is formed by three main steep, ESE- or SE-facing range fronts that step left in an en echelon fashion (Fig. 1b). In addition, a small emerging ridge, called Little Rough Ridge, outcrops parallel to and 4 km southeast of the northernmost major segment (North Rough Ridge). All the ridges are anticlines in the peneplain surface. Cotton (1917, 1919) noted these stepping ridges, which he described as a 'splintered fault scarp', though in reality there is little evidence for faulting at the surface.

Oliverburn Step

Figures 5(a) and 8 show the drainage pattern in the region of the southernmost step in the Rough Ridge system at Oliverburn. The topography consists of the high drainage divide of Rough Ridge at ~1000 m elevation with a lower (~700 m high) parallel ridge about 3 km to the east. The lower frontal ridge, which we informally refer to here as 'South Rough Ridge', loses elevation towards the north and eventually merges with the Upper Taieri plain at a height of ~460 m near Oliverburn (Fig. 5b). Sarsen stones are still found at the low northern end of the frontal ridge, confirming that

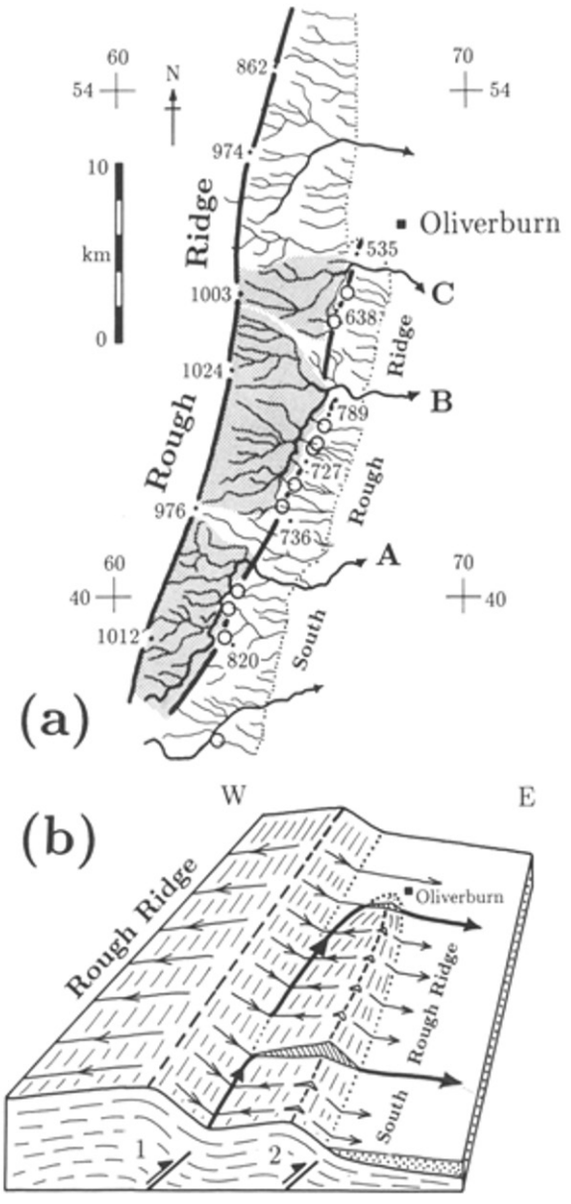

Fig. 8. Drainage map of the step in the range front between South Rough Ridge and Rough Ridge at Oliverburn (see Fig. 1). The catchments of streams A, B and C are shaded. Symbols as in Fig. 2, with air gaps marked by open circles. (b) Schematic cartoon illustrating the structure and drainage in (a). Note the dry air gaps on the frontal ridge. The gathering of the major streams into asymmetric catchments that cross South Rough Ridge suggests that the fault underlying it (2) is later than the one forming Rough Ridge (1), and propagated to the north.

the topography is essentially a warping of the peneplain surface and not formed by erosion.

The drainage pattern is simple and informative. Three large streams (marked A–C in Fig. 8a) cross the divide of South Rough Ridge in gorges. All of them have extremely asymmetric catchments, with virtually all the drainage in them arising from south of where they cross the South Rough Ridge divide. The reason for this pattern is clear: the South Rough Ridge divide contains numerous dry air gaps (open circles in Fig. 8a) that mark where streams used to flow from the high Rough Ridge divide in the west across what is now the frontal divide of South Rough Ridge. These streams have been diverted by the emerging South Rough Ridge and their catchments gathered together until they achieve an erosive

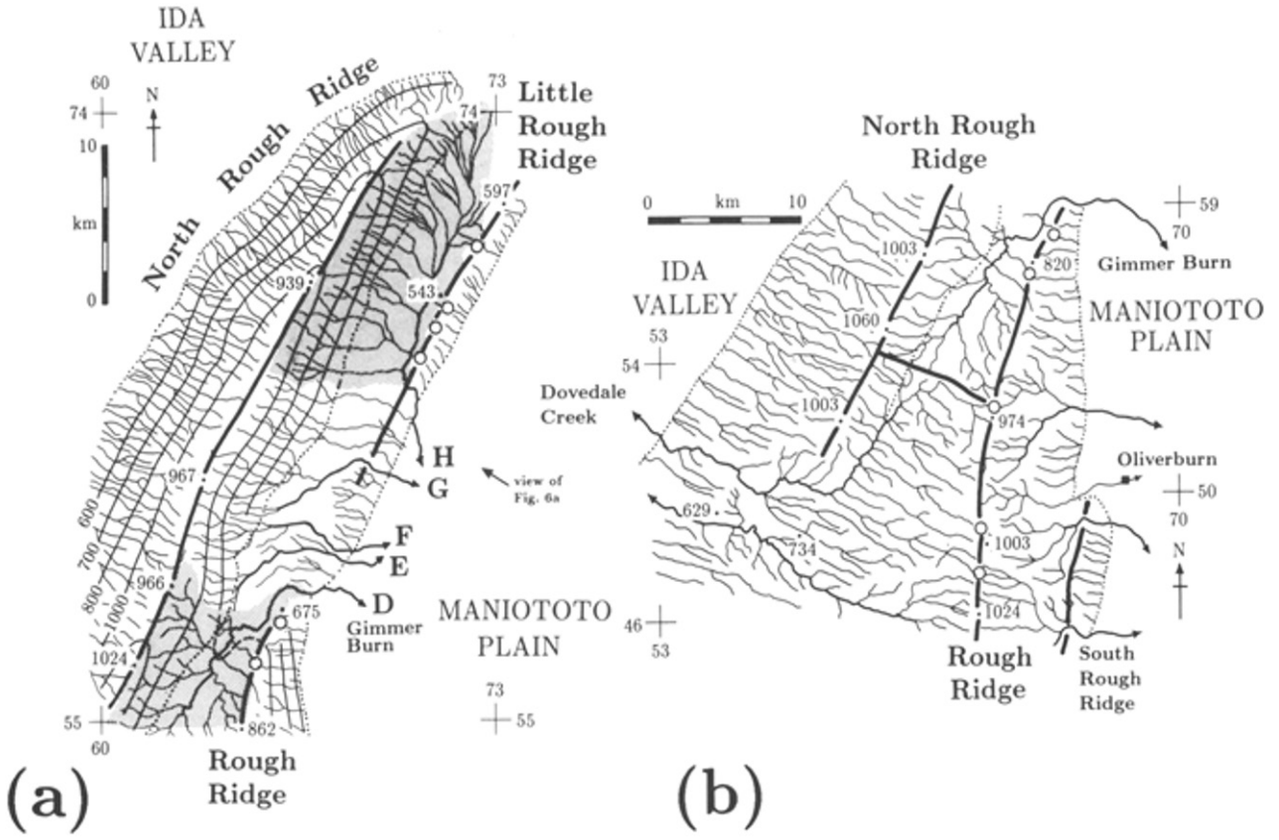

Fig. 9. (a) Drainage and structural contour map for the North Rough Ridge–Little Rough Ridge region (see Fig. 1). Symbols as in Fig. 2, with air gaps marked by open circles. Major catchments are shaded. (b) Drainage map of the southern end of North Rough Ridge. Symbols as in (a).

power sufficient to maintain their courses across or round the end of the anticline. Thus South Rough Ridge clearly formed later than the higher Rough Ridge to the northwest, and the asymmetry of the catchments indicates that it propagated towards the northeast as it grew.

Gimmer Burn Step

The high drainage divide of Rough Ridge continues north of the region in Fig. 8(a), dropping gradually in elevation to about 700 m. Near Gimmer Burn (stream D in Fig. 9a) it starts to become indistinct, merging with the much lower (~550 m) Little Rough Ridge that joins it obliquely from the northeast (Fig. 10a). Gimmer Burn occupies a step to the left between the Rough Ridge and North Rough Ridge drainage divides.

Rough Ridge runs N–S, oblique to both the stream courses west of it and to the higher (900–1000 m) North Rough Ridge. On the other hand, the drainage divide on North Rough Ridge is perpendicular to the streams on both its flanks and those streams are also perpendicular to the structural contours on the peneplain surface (Fig. 9a). Three large streams (D–F in Fig. 8b) cross the northern nose of Rough Ridge in gorges. All of them are convex to the north and have asymmetric catchments collecting drainage from the south of their gorges. The north end of the Rough Ridge drainage divide contains two dry air gaps (open circles in Fig. 9a) that appear to have been formed by streams that used to drain southeast off North Rough Ridge, but now drain northwest off Rough Ridge into Gimmer Burn. These air gaps and the asymmetry of the catchments of streams D–F suggest that, in the Gimmer Burn region, Rough Ridge grew after North Rough Ridge had already established its consequent drainage pattern. As Rough Ridge propagated north the streams that used to cross its line were deflected north and having gathered sufficient catchment could maintain their arcuate course around the nose of the propagating anticline. It is difficult to see how this could happen, and especially how the arcuate stream courses could develop, if the southwest end of Little Rough Ridge was already formed (see later).

Gimmer Burn itself (stream D in Fig. 9a) exhibits incised meanders in the sections of its course west of the two air gaps at the northern end of Rough Ridge (Figs. 6b and 9a). The meanders presumably developed in response to reduced stream gradients against the rising and propagating Rough Ridge. Once the river established itself across the axis of Rough Ridge subsequent downcutting of the stream through the growing structure preserved the meanders.

North Rough Ridge–Little Rough Ridge

Little Rough Ridge (Fig. 6) is younger than the much higher North Rough Ridge. Along its drainage divide it contains several air gaps (open circles in Fig. 9a), some of which are now occupied by small lakes. These gaps mark the former courses of streams flowing off North Rough Ridge, most of which are now gathered into the

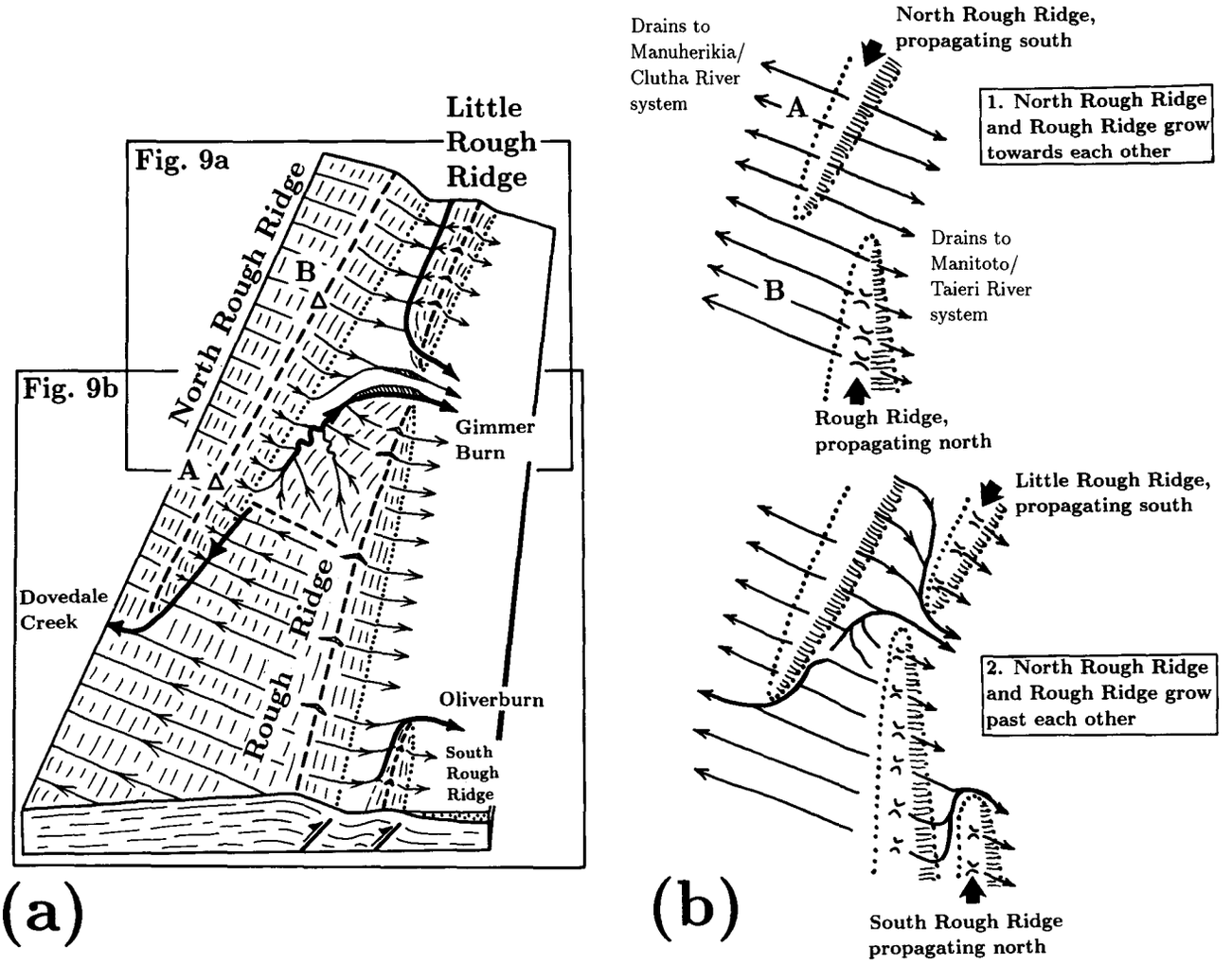

Fig. 10. (a) Schematic cartoon illustrating the structure and drainage in Fig. 9. The highest point on North Rough Ridge is at A, though the greatest scarp height is further north at B. (b) Schematic evolution of the structures and drainage in (a). In the region A the drainage is probably consequent on the development of North Rough Ridge. We are less sure about the region B: here some features of the drainage, such as its obliquity to the Rough Ridge divide and some air gaps on the divide itself suggest that the drainage may pre-date the development of Rough Ridge, but there is no obvious source for such a closely-spaced antecedent pattern.

catchment which crosses Little Rough Ridge in stream H in Fig. 9(a). Northwest of Little Rough Ridge stream H has now cut 20 m or more below the abandoned lakes and marshes in the air gaps. The asymmetry of the catchment area in stream H suggests that Little Rough Ridge grew by propagation to the southwest. We have already suggested that the northern end of Rough Ridge formed earlier than the southwest end of Little Rough Ridge, so that the arcuate courses of streams D–F could develop. Those stream courses have some additional curious features. They flow in valleys that are asymmetric, with steeper northern sides than southern. This is to be expected if they have remained in place during a tilting to the north as the nose of Rough Ridge was uplifted. Streams E–G flow in gorges across the line of the Little Rough Ridge divide, but only in their lower reaches, as they cross the divide itself, are those gorges still incising. Farther upstream, on the northwest side of the frontal divide, the streams occupy old V-shaped valleys that now have broad flat bottoms (Fig. 6b): in other words the upstream valleys have changed from sites of incision to deposition. We speculate that this change arose when the gorges, which were cut into the propagating and uplifting nose of Rough Ridge, had their profiles warped by the later emerging Little Rough Ridge. This would have steepened the downstream gradient of the streams but lessened the upstream gradients. This interpretation is consistent with the southwest end of Little Rough Ridge post-dating the northern end of Rough Ridge.

The region between streams F and H is a subdued and gentle saddle in the divide of Little Rough Ridge, occupied by stream H. Here the asymmetry of the catchment areas crossing the frontal divide reverses, and we are unsure whether the Little Rough Ridge anticline represents one or two fault segments at depth.

Evolution of the Rough Ridge system

Clues to the general evolution of the Rough Ridge system are preserved near the southern end of North Rough Ridge (Fig. 9b). Here the drainage pattern changes dramatically across a NW–SE-trending divide that separates the headwaters of Gimmer Burn (which flows north) from those of Dovedale Creek (which flows south) and joins North Rough Ridge to Rough Ridge.

South of this transverse divide is a strong linear SE–NW drainage system that continues a further 15 km south of Fig. 9(b). This linear drainage system flows northwest of Rough Ridge but is blocked at the southern end of North Rough Ridge and diverted into Dovedale Creek, which flows round the end of the North Rough Ridge escarpment. Thus, in this region, North Rough Ridge is younger than the SE–NW drainage system.

Near the Gimmer Burn gorge we have already established that Rough Ridge is younger than the SE-flowing drainage coming off North Rough Ridge. But near the transverse divide at the head of Dovedale Creek (Fig. 9b), Rough Ridge presumably is older than North Rough Ridge, or the drainage here would flow to the southeast, crossing Rough Ridge, as it does farther north. Thus, we conclude that in this region the northward-propagating Rough Ridge and the southward-propagating North Rough Ridge grew towards each other, disturbing the SE–NW drainage pattern (Fig. 10b). The two ridges met in the region of the transverse divide at the headwaters of Dovedale Creek and Gimmer Burn. Unlike the Raggedy Ridge and Blackstone Hill faults they did not coalesce but grew past each other.

Two other features are significant. First, the highest point on North Rough Ridge (1060 m) is by the transverse divide (Fig. 9a), but this is not the greatest relief across the North Rough Ridge scarp, which occurs farther north, opposite streams E–H in Fig. 9(a). This scarp height decreases southwards, but the maximum elevation of the ridge crest is achieved at the transverse divide with help from the uplift of Rough Ridge to the east. Second, the linear SE–NW drainage pattern is lost in the headwaters of Gimmer Burn, north of the transverse divide (Fig. 9b). The pattern there looks more like a radial pattern superimposed on the propagating nose of Rough Ridge. In this region (unlike south of the transverse divide) Rough Ridge was propagating into the SE-flowing drainage off North Rough Ridge and diverting it north against the regional trend of the axial drainage, which is to the south. This may be responsible for the gentle axial gradients in the headwaters of Gimmer Burn, leading to the formation of meanders (now incised). In these circumstances, it may have been possible to establish a radial drainage pattern on the nose of Rough Ridge.

These relations are summarized in Fig. 10. It is clear that the Rough Ridge system is not underlain by a single continuous fault at depth, and that the discontinuities at the surface reflect the evolution of quite separate underlying fault segments. The general evolution of the system consists of two S-propagating (North Rough Ridge and Little Rough Ridge) and two N-propagating ridges (Rough Ridge and South Rough Ridge). North Rough Ridge and Rough Ridge are the two oldest, and grew towards each other. The drainage pattern in the central (and highest relief) section of North Rough Ridge is perpendicular to the divide and to the structural contours on the peneplain surface (Fig. 9a) and may be consequent on North Rough Ridge itself. These two ridges propagated past each other near the current headwaters of Dovedale Creek and Gimmer Burn. Both Little Rough Ridge and the frontal ridge at Oliverburn are younger than Rough Ridge, but their relative ages cannot be distinguished. Once again, we caution that we cannot as yet distinguish relative ages from relative rates of uplift.

QUANTITATIVE GROWTH RATES

So far we have restricted ourselves to qualitative arguments about fault growth and interaction. There is some potential for quantitative estimates, but these require additional work. One possibility is the use of river terraces. Regional uplift has caused many of the longitudinal river valleys to become terraced, and many of the terrace surfaces are large in areal extent and easily identified. These terraces are in turn uplifted, accentuated and deformed locally by emerging range fronts. These offer the potential for quantitative estimates of uplift and propagation rates, but the terraces have not yet been satisfactorily dated.

Another possibility is offered by the shapes or profiles of old river courses in air gaps. This requires more detailed topographic data than are currently available, but a simple example will illustrate the possibilities. The large dry river course in the air gap south of the Ida Burn gorge in Fig. 7 is 100 m above the abandoned entrance to this old gorge. Since the old entrance is at roughly the height of the presently flowing gorge we surmise that the channel has suffered around 100 m uplift during the time the Raggedy Range fold has propagated about 3 km to the northeast. The fold itself is about 20 km long, and we assume is underlain by a steep reverse fault of roughly the same length. If, like Jackson & Leeder (1994), we assume that the fault moves only in earthquakes that rupture the total available fault length, then a fault 20 km long would be expected to move about 1–2 m in each earthquake (e.g. Scholz 1982). This estimate of incremental slip is similar to that found in trenches across other faults of similar size in the region (e.g. Beanland & Berryman 1991, Norris *et al.* 1994). Allowing for fault dip (say ~45°) and the likelihood that the fault displacement dies out near the surface, this may produce around 0.5–1.0 m uplift of the hangingwall. Thus 100 m uplift would require the order of 100–200 earthquakes, during which time the fault propagated 3 km: giving a propagation rate of 15–30 m per earthquake.

The same reasoning may be applied to other gorges and air gaps in the examples cited here. The results are summarized in Table 1, and all give propagation rates in the region of 10–50 m per earthquake. These are not estimates to take too seriously: they are built on an edifice of assumptions each of which can be questioned and is uncertain. However, they are not ludicrous. They are similar to the 30–50 m per earthquake estimated in Nevada for a normal fault of similar length by Jackson & Leeder (1994), which in turn is within the range of fault growth rates predicted for faults of this length by theor-

Table 1. Gorges and air gaps that have been used to estimate ridge propagation rates. We estimate that these features have been uplifted a height H while the ridge propagated a distance L. This propagation required an estimated N earthquakes, yielding a propagation rate in m per event given in the last column

Structure	Location	H (m)	L (m)	N	m per event
Raggedy Ridge	Air gap at 655N 510E	100	3000	100–200	15–30
Rough Ridge	Gimmer Burn gorge 591 663	200	7000	200–400	18–35
	Omnibus Creek 610 670	100	4500	100–200	23–45
	Gorge at 630 685	40	1500	40–80	19–38
South Rough Ridge	Waitoi Creek 458 665	160	4000	160–320	13–25
	Dingo Creek 490 674	50	1500	50–100	15–30

etical growth models (Walsh & Watterson 1988, Cowie & Scholz 1992). With our existing data we regard anything more sophisticated as premature.

DISCUSSION

This study has demonstrated that the drainage systems associated with active folds and reverse faults can contain information about the growth and interaction of those structures. We have seen how asymmetric folds can evolve into box-like folds (Taieri Ridge and the Rock and Pillar Range); that apparently continuous ridges can be shown to have formed from separately evolving fault segments that coalesced (Raggedy Range–Blackstone Hill); several examples where the relative ages (or uplift rates) of ridges can be distinguished; and evidence for the propagation direction of folds (or faults) as they grow. We attach greater significance to the fact that we can detect these processes in action than to the generalization of any results from such a limited study. For instance, we have seen that the highest ridges are also apparently the earliest formed (or the most rapidly uplifting), and that the youngest ridges have evidently formed in front of older ones (i.e. in the footwalls of the underlying reverse faults). These apparent generalizations may not be significant: it may simply be that these arrangements are easier to recognize than others.

However, we can identify several general features of the drainage that are useful to identify or consider.

(1) Is the drainage divide (or fold axis) perpendicular to the stream systems on the flanks? If it is, as on Taieri Ridge (Fig. 2a), then the stream system is likely to be consequent on the ridge development. If not, the stream system may be antecedent, predating the growth of the ridge (the northern end of Rough Ridge (Fig. 9a) is a possible example).

(2) Is the asymmetry of the drainage mirrored in the asymmetry of the topography? In simple structures such as Taieri Ridge (Fig. 2a) this is usually the case. If it isn't, such as in the Rock and Pillar Range (Fig. 2b), there may be a simple structural explanation.

(3) The position of air gaps on drainage divides may be significant for ascertaining both the relative ages (or activities) of structures and their directions of propagation.

(4) Where antecedent streams cross ridges in gorges the asymmetry of their catchment areas upstream may indicate the direction of propagation of the ridge, as in South Rough Ridge (Fig. 8a).

(5) Longitudinal stream courses may also contain clues to fault growth and interaction, particularly if they flow against the regional drainage trend (such as Pool Burn in Fig. 7a) or incise through other structures (such as the Manuherikia River in the Lauder gorge).

This study has raised a number of new questions. The gathering of abandoned antecedent streams into large asymmetric catchments that then maintain gorges through ridges, as in Figs. 8 and 9, is a particularly striking feature of the drainage. It is natural to ask what controls the gathering process. The pattern itself is most pronounced in the early stages of ridge growth: thus Little Rough Ridge (Fig. 9a), and the ridge south of Oliverburn (Fig. 8a) have several streams that cut through the drainage divide, whereas the Raggedy Range–Blackstone Hill ridge is now reduced to one. It may be that nearly all the streams are eventually captured by a single dominant one: if this is so, what controls the position of the successful stream? The Ida Burn gorge through the Raggedy Range is located in the logical last opportunity for such a stream after it has captured all the others: i.e. in a structural low or saddle formed where two fault segments have propagated towards each other and met. But this may not always be the case.

A major issue raised by this study is the interaction between fault growth, earthquake recurrence rates and climatic change. A growth of 50 m per earthquake may not sound much, but when combined with earthquake recurrence intervals of a few thousand years (e.g. Berryman & Beanland 1991) it is easy to see how ridges might grow a few km during a major climatic cycle of 100,000 years. Rivers might be able to establish their courses round the ends of ridges during wet periods but be unable to maintain smaller streams in gorges through growing ridges in relatively dry periods. If so, then the next stream channel to be established across the ridge may form at the point reached by the end of the propagating ridge at the start of the next wet period. Could this be responsible for the semi-regular spacing of the successful streams crossing South Rough Ridge south of Oliverburn in Fig. 8(a)? But such a pattern might be expected even if the climate were constant, on the grounds that the catchments simply need to acquire sufficient area, and hence erosive power, to maintain

their gorge through the ridge. To address such questions we require more information about the local climatic changes associated with global sea level fluctuations and also some constraint on timing.

CONCLUSIONS

We have demonstrated that drainage patterns in a region of active shortening are able to reveal aspects of fault (and fold) growth and interaction that would be very difficult to obtain by other means. In particular we have seen: (1) how asymmetric folds can develop into box folds; (2) how apparently continuous ridges may in fact have formed from the meeting of two quite distinct fault segments that grew towards each other; (3) evidence for the relative ages (or uplift rates) on adjacent structures; and (4) evidence for the direction of propagation of ridges and their underlying reverse faults as they grow. Central Otago is ideal for this purpose as it has a well-developed peneplain surface that can be used as a marker and moreover is cut into the same rock type all over the region, so that the topographic variations are mostly related to structure rather than to differential erosion. However, there is no reason to think that the processes we see revealed in central Otago are peculiar to that region: they are likely to occur everywhere, but may be harder to recognize. For example, Ollier (1981) gives some similar interpretations of larger-scale river patterns in regions of Australia that are now tectonically inactive.

With the existing data, this study has necessarily been qualitative. The quantitative estimates we obtained for ridge (or fault) propagation of ~10–50 m per earthquake for a structure ~20 km in length are very uncertain, but similar to an estimate made for a normal fault of similar length in Nevada and similar also to the predictions of theoretical models. Growth rates of this magnitude, combined with earthquake recurrence intervals of order 1000 years, are able to propagate structures a few km during a major 100,000 year sea level and climate cycle. This raises the issue of the extent to which fault growth, earthquake recurrence rates and climate change interact to produce discrete or even semi-regular features in the drainage of a tectonically active landscape, such as the spacing of antecedent gorges through emerging ridges. While theoretically this interaction is plausible, lack of hard evidence means that, for the moment, it remains speculative.

Acknowledgements—We thank D. Prior and R. Knipe for generous and helpful reviews. J. Jackson thanks the Institute of Geological and Nuclear Sciences for support in New Zealand. This is Cambridge Earth Sciences contribution 4316. R. Norris and J. Youngson acknowledge financial support from the University of Otago and from the NZ Foundation for Research, Science and Technology.

REFERENCES

Beanland, S. & Barrow-Hurlbert, S. A. 1988. The Nevis–Cardrona fault system, central Otago, New Zealand: Late Quaternary tectonics and structural development. *N.Z. J. Geol. Geophys.* **31**, 337–352.

Beanland, S. & Berryman, K. R. 1989. Style and episodicity of late Quaternary activity on the Pisa–Grandview fault zone, central Otago, New Zealand. *N. Z. J. Geol. Geophys.* **32**, 451–461.

Beanland, S., Berryman, K. R., Hull, A. G. & Wood, P. R. 1986. Late Quaternary deformation at the Dunstan Fault, central Otago, New Zealand. *R. Soc. N.Z. Bull.* **24**, 293–306.

Berryman, K. R. & Beanland, S. 1991. Variation in fault behaviour in different tectonic provinces of New Zealand. *J. Struct. Geol.* **13**, 177–189.

Berryman, K. R., Beanland, S., Cooper, A. F., Cutten, H. N., Norris, R. J. & Wood, P. R. 1992. The Alpine Fault, New Zealand: variation in Quaternary structural style and geomorphic expression. *Ann. Tecton.* **6**, 126–163.

Bishop, D. G. 1974. Stratigraphic, structural and metamorphic relationships in the Dansey Pass area, Otago, New Zealand. *N.Z. J. Geol. Geophys.* **17**, 301–335.

Bishop, D. G. 1994. Extent and regional deformation of the Otago peneplain. Institute of Geol. Nuclear Sciences, Science report 94/1.

Cotton, C. A. 1917. Block mountains in New Zealand. *Am. J. Sci.* **44**, 249–293.

Cotton, C. A. 1919. Rough Ridge, Otago, and its splintered fault scarp. *Trans. N.Z. Inst.* **51**, 282–285.

Cotton, C. A. 1942. *Geomorphology* (3rd edn). Whitcombe & Tombs Ltd, Christchurch, New Zealand.

Cowie, P. A. & Scholz, C. H. 1992. Growth of faults by accumulation of seismic slip. *J. geophys. Res.* **97**, 11,085–11,095.

Crone, A. J. & Haller, K. M. 1991. Segmentation and the coseismic behaviour of Basin and Range normal faults: examples from east-central Idaho and southwestern Montana, U.S.A. *J. Struct. Geol.* **13**, 151–164.

Dawers, N. H. & Anders, M. H. 1995. Displacement-length scaling and fault linkage. *J. Struct. Geol.* **17**, 607–614.

Gillespie, P. A., Walsh, J. J. & Watterson, J. 1992. Limitations of dimension and displacement data from single faults and the consequences for data analysis and interpretation. *J. Struct. Geol.* **14**, 1157–1172.

Hauksson, E. *et al.* (+18 co-authors) 1988. The 1987 Whittier Narrows earthquake in the Los Angeles metropolitan area, California. *Science* **239**, 1409–1412.

Jackson, J. A. & Leeder, M. R. 1994. Drainage systems and the development of normal faults: an example from Pleasant Valley, Nevada. *J. Struct. Geol.* **16**, 1041–1059.

King, G. & Vita-Finzi, C. 1981. Active folding in the Algerian earthquake of 10 October 1980. *Nature* **292**, 22–26.

Leeder, M. R. & Gawthorpe, R. L. 1987. Sedimentary models for extensional tilt-block/half-graben basins. In: *Continental Extensional Tectonics* (edited by Coward, M. P., Dewey, J. F. & Hancock, P. L.). *Spec. Publs geol. Soc. Lond.* **28**, 139–152.

Leeder, M. R. & Jackson, J. A. 1993. The interaction between normal faulting and drainage in active extensional basins, with examples from the western United States and central Greece. *Basin Res.* **5**, 79–102.

McCraw, J. D. 1965. Landscapes of Central Otago. In: *Central Otago. A Symposium to Mark the Centenary of the "Golden Decade" of the 1860s in Central Otago* (edited by Lister, R. G. & Hargreaves, R. P.). New Zealand Geographical Society, 30–45.

McSaveney, M. J. & Stirling, M. W. 1992. Central Otago: Basin and Range country. In: *Landforms of New Zealand* (edited by Soons, J. M. & Selby, M. J.). Longman Paul, New Zealand, 482–504.

Madin, I. 1988. Geology and neotectonics of the Upper Manuherikia basin, central Otago, New Zealand. *N.Z. Geol. Surv. Rec.* **27**.

Molnar, P. & Chen, W-P. 1982. Seismicity and mountain building. In: *Mountain Building Processes* (edited by Hsu, K. J.). Academic Press, New York, 41–57.

Mortimer, N. 1993. Geology of the Otago Schist and adjacent rocks. Scale 1:500,000. *Inst. Geol. Nuclear Sci. Geological Map* 7. Inst. Geol. Nuclear Sci. Ltd., Lower Hutt, New Zealand.

Norris, R. J., Koons, P. O. & Cooper, A. F. 1990. The obliquely-convergent plate boundary in the South Island of New Zealand: implications for ancient collision zones. *J. Struct. Geol.* **12**, 715–725.

Norris, R. J., Koons, P. O. & Landis, C. A. 1994. Seismotectonic evaluation of fault structures in eastern Otago. Report 91/53, Earthquake Commission New Zealand.

Ollier, C. 1981. *Tectonics and Landforms*. Longman, London, 164–174.

Pacheco, J. F., Eastbrook, C. H., Simpson, D. W. & Nabalek, J. L. 1989. Teleseismic body wave analysis of the 1988 Armenian earthquake. *Geophys. Res. Lett.* **16**, 1425–1428.

Philip, H., Rogozhin, E., Cisternas, A., Bousquet, J. C., Borisov, B. & Karakhanian, A. 1992. The Armenian earthquake of 1988 December 7: faulting and folding, neotectonics and paleoseismicity. *Geophys. J. Int.* **110**, 141–158.

Roberts, S. & Jackson, J. A. 1991. Active normal faulting in central Greece: an overview. In: *The Geometry of Normal Faults* (edited by Roberts, A. M., Yielding, G. & Freeman, B.). *Spec. Publs geol. Soc. Lond.* **56**, 125–142.

Ruegg, J. C., Kasser, J. C., Tarantola, A., Lepine, J. C. & Chouikrat, B. 1982. Deformations associated with the El Asnam earthquake of 10 October 1980: geodetic determination of vertical and horizontal movements. *Bull. seism. Soc. Am.* **72**, 2227–2244.

Salton, G. 1993. Mechanics of folding in central Otago: an investigation of the Recent deformation of the Rock and Pillar Range. Unpublished M.Sc. thesis, University of Otago.

Scholz, C. H. 1982. Scaling laws for large earthquakes: consequences for physical models. *Bull. seism. Soc. Am.* **72**, 1–14.

Scholz, C. H., Dawers, N. H., Yu, I. Z. & Anders, M. H. 1993. Fault growth and scaling laws: preliminary results. *J. geophys. Res.* **98**, 21,951–21,961.

Schwartz, D. P. & Coppersmith, K. J. 1984. Fault behaviour and characteristic earthquakes: examples from the Wasatch and San Andreas fault zones. *J. geophys. Res.* **89**, 5681–5698.

Shimazaki, K. 1986. Small and large earthquakes: the effects of the thickness of the seismogenic layer and the free surface. In: *Earthquake Source Mechanics* (edited by Das, S., Boatwright, J. & Scholz, C. H.). *Am. Geophys. Un. Geophys. Monogr.* **37**, 209–216.

Stein, R. S. & King, G. 1984. Seismic potential revealed by surface folding: 1983 Coalinga, California, earthquake. *Science* **224**, 867–872.

Stein, R. & Yeats, R. 1989. Hidden earthquakes. *Scient. Am.* **260**, 48–57.

Stirling, M. W. 1990. The Old Man and Garvie mountains: tectonic geomorphology of the central Otago peneplain, New Zealand. *N.Z. J. Geol. Geophys.* **33**, 233–243.

Suggate, R. P. 1978. The Late Mobile phase: Cretaceous. In: *The Geology of New Zealand, Vol.* 2 (edited by Suggate, R. P., Stevens, G. R. & Te Punga, M. T.). Government Printers, New Zealand.

Trudgill, B. & Cartwright, J. 1994. Relay-ramp forms and normal-fault linkages, Canyonlands National Park, Utah. *Bull. geol. Soc. Am.* **106**, 1143–1157.

Walsh, J. & Watterson, J. 1988. Analysis of the relationship between displacements and dimensions of faults. *J. Struct. Geol.* **10**, 239–247.

Watterson, J. 1986. Fault dimensions, displacements and growth. *Pure & Appl. Geophys.* **124**, 365–373.

Wu, D. & Bruhn, R. L. 1994. Geometry and kinematics of active normal faults, South Oquirrh mountains, Utah: implication for fault growth. *J. Struct. Geol.* **16**, 1061–1075.

Yeats, R. S. 1986. Active folds related to folding. In: *Active Tectonics* (edited by R. E. Wallace). National Academy Press, Washington, DC, 63–79.

Yeats, R. S. 1987. Tectonic map of central Otago based on Landsat imagery. *N.Z. J. Geol. Geophys.* **30**, 261–271.

Yielding, G. 1985. Control of rupture by fault geometry during the 1980 El Asnam (Algeria) earthquake. *Geophys. J. R. astr. Soc.* **81**, 641–670.